Creation of the first high-inductance sensor of the CCC-Sm series

HELMHOLTZ
Helmholtz-Institut Jena

V. Tympel[1,2], T. Stöhlker[1,2,3], F. Machalett[3], M. Stapelfeld[4], T. Schönau[4], F. Schmidl[4], P. Seidel[4], L. Crescimbeni[2], D. Haider[2], M. Schwickert[2], T. Sieber[2], M. Schmelz[5], R. Stolz[5], V. Zakosarenko[5,6]

[1] Helmholtz Institute Jena (HI-Jena), Germany; [2] GSI Helmholtz Center for Heavy Ion Research, Darmstadt, Germany; [3] Institute for Optics and Quantum Electronics (IOQ), 07743 Jena, Germany; [4] Institute of Solid State Physics (IFK), 07743 Jena, Germany, [5]Leibniz Institute of Photonic Technology (IPHT), 07745 Jena, Germany; [6] Supracon AG, 07751 Jena, Germany;

Abstract

Cryogenic Current Comparators (CCC) for beamlines are presently used at CERN-AD and in the FAIR project at CRYRING with 100 mm and 150 mm beamline diameter, respectively, for non-destructive absolute measurement of beam currents in the amplitude range of below 10 μA_{pp} (current resolution 1 nA_{pp}). Both sensor versions (CERN-Nb-CCC and FAIR-Nb-CCC-XD) use niobium as a superconductor for the DC-transformer and magnetic shielding. The integrated flux concentrators have an inductance below 100 µH at 4.2 Kelvin. The new Sm-series (Smart & Small) is designed for a beamline diameter of 63 mm and is using lead (Pb) as superconductor. The first implemented sensor (IFK-Pb-DCCC-Sm-200) has two core-based pickup coils (2 x 100 µH at 4.2 K) and hence the option to use two SQUID units. During construction, some basic investigations such as on noise behavior (fluctuation–dissipation theorem, white noise below 2 $pA_{rms}/\sqrt{Hz}$) and the magnetic shielding in terms of L_{core}-$C_{meander}$-resonance and additional mu-metal shielding were undertaken. These results are presented herein. Finally, a current resolution of 0.5 nA_{pp} was achieved without additional shielding measures in laboratory environment.

Introduction

Cryogenic Current Comparators (CCC) measure the azimuthal magnetic field of a charged particle beam non-destructively (see Fig. 1). By using superconducting components such as magnetic shielding, DC transformer, and SQUIDs, a current resolution in the nA range can be achieved [1]. After the development of large CCCs for the CERN Antiproton Decelerator (CERN-Nb-CCC) [2] and FAIR-project (FAIR-Nb-CCC-XD) [3], both with a current pulse resolution >1 nA, some new concepts are currently being tested on smaller size CCCs - the so-called Small & Smart series (CCC-Sm, <1 nA).

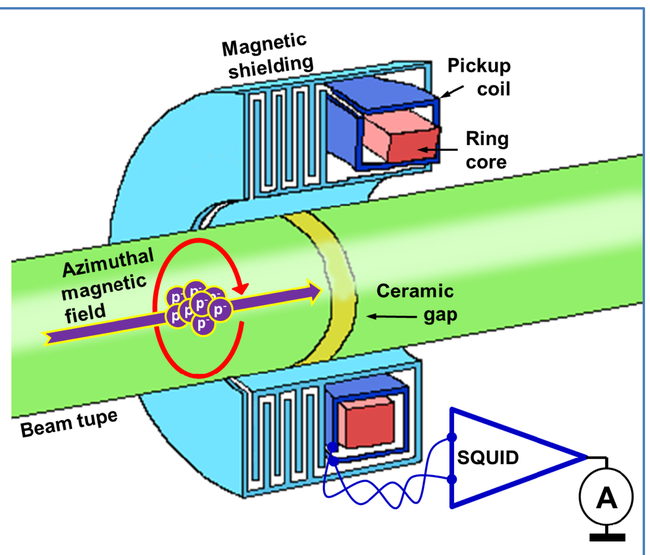

Figure 1: Classical CCC design for beamlines. [4]

Pickup coils

To increase system availability and enable comparison experiments, the setup is carried out with two superconductive pickup coils (Dual-core CCC or DCCC). Standard Magnetec M-616 cores [5] were used for the first DCCC-Sm (see Fig. 2), which achieve an inductance of about 100 µH in a package of three cores per coil (see Fig. 3).

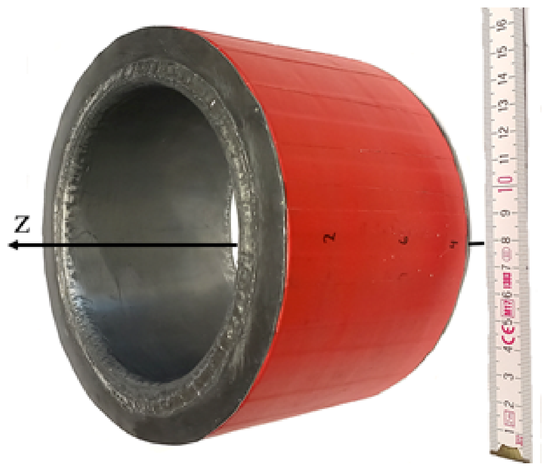

Figure 2: Pickup coil #1, one full-faced single-turn coil made of lead through three M-616 cores with z-axis as later beam direction.

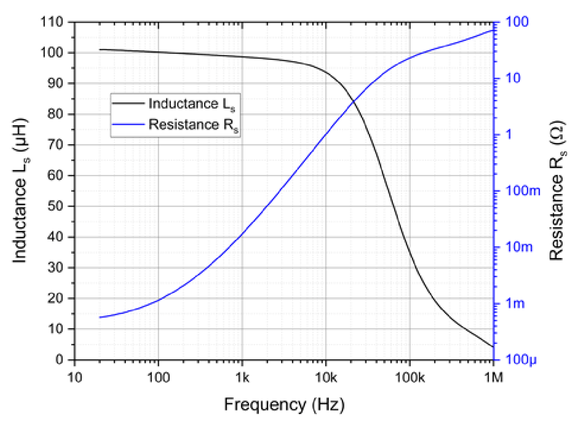

Figure 3: Pickup coil #1, serial inductance Ls and serial resistance R_s measured at 4.2 K.

Fluctuation-Dissipation Theorem

Following the fluctuation-dissipation theorem (FDT), an expected value for the current noise density $i_{rms}/\sqrt{(\Delta f)}$ can be calculated by the serial inductance L_s and the serial resistance R_s of the pickup coil as functions of the frequency f, the fixed input coil inductance L_i (1 µH) of the SQUID, at a fixed temperature T (4.2 K) and a fixed frequency interval Δf, shown in Eq. (1) [6]:

$$\frac{{i_{rms}}^2}{\Delta f} = 4k_B T \cdot \frac{R_s(f)}{\left(2\pi f \cdot (L_i + L_s(f))\right)^2 + \left(R_s(f)\right)^2} \qquad (1)$$

Figure 4 shows the good agreement of the directly measured spectral current noise density with the calculation via the FDT in the white noise range > 1 kHz. The slight overestimation of the current noise density in the frequency range < 1 kHz (1/f noise) may be due to a systematic error in determining the resistance R_s (< 10 mΩ) for low frequencies.

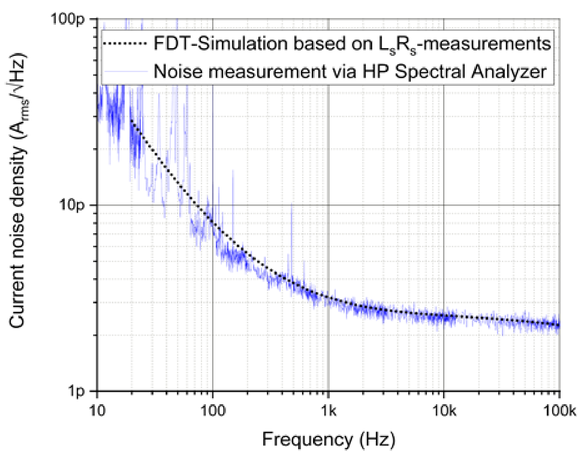

Figure 4: Pickup coil #1, spectral current noise density.

Dual-core CCC

Two pickup coils then have been equipped with common superconducting shielding against magnetic interference signals (Fig. 5).

Magnetic Shielding & LC-Resonances

The shielding consists of two superconductive coaxial tubes comprising the pickup coils connected to each other at one end. The longer the tube package, the better the suppression of interference signals. Since long tubes would be impractical, the tubes are folded into a meander structure.
The opposite surfaces of the meander structure also form an electrical capacitance $C_{meander}$, which increases with increasing number of meanders or effective length of the tube package. The inner loop (see Fig. 5 left) creates an inductance L_{core}, which together with $C_{meander}$ forms a parallel LC-resonance circuit. Figure 6 shows the shift of the meander LC-resonance measured via the current noise density with 2, 6, and finally 12 (240 cm) full meander pairs.

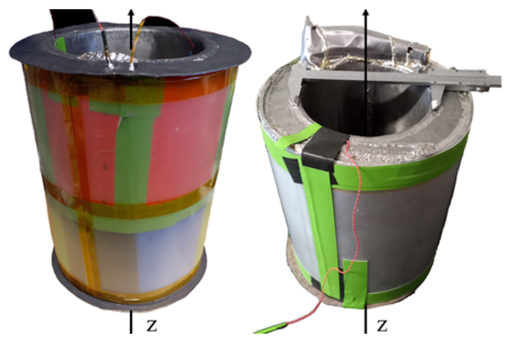

Figure 5: Left: Pickup coils #1 and #2 with inner loop of the shielding. Right: DCCC completed by the outer meander shielding, SQUID and calibration coil.

Current Noise & Current Pulses

The noise measurements were carried out in the frequency range < 100 kHz with a HP 35670A and up to 5 MHz with a HP 89410A (see Fig. 7). An additional calibration coil and a certified multimeter Keithley 2002 were used for current calibration. The high frequency range above 100 kHz is determined by the discussed meander LC-resonance and the frequency limitation of the core material. The medium frequency range (1 kHz to 100 kHz) has a close to constant noise behavior (white noise). With minimal 1.7 $pA_{rms}/\sqrt{Hz}$) the absolute values are $1/\sqrt{2}$ times smaller than values from the FDT studies, exactly as expected.

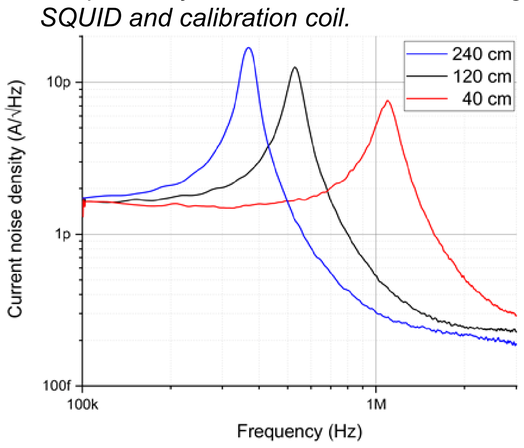

Figure 6: LC-resonance peaks of the DCCC-Sm-200 at three processing stages with increasing number of meander pairs or effective length of the shielding tube package.

A parallel connection of both pickup coils leads to an increase in noise, which is describable with the Pythagorean addition of the single independent noise sources. The low frequency range < 1 kHz shows a significant increase in noise density, which ultimately (< 1 Hz) results in a 1/f2 behavior, as it leads to Brownian noise. In addition, in the range between 3 Hz and 80 Hz, other interference signals become visible, most of which can be traced back to building vibrations.

Measurements were performed by application of defined current pulses on the calibration coil (single wire through the DCCC). Figure 8 shows the 500 pA current pulses to be measured (dotted line) and the SQUID responses (blue line), smoothed with a 10 kHz low-pass filter and calibrated to current values. For similar measurements, the FAIR-Nb-CCC-XD required 1.6 nA current pulses.

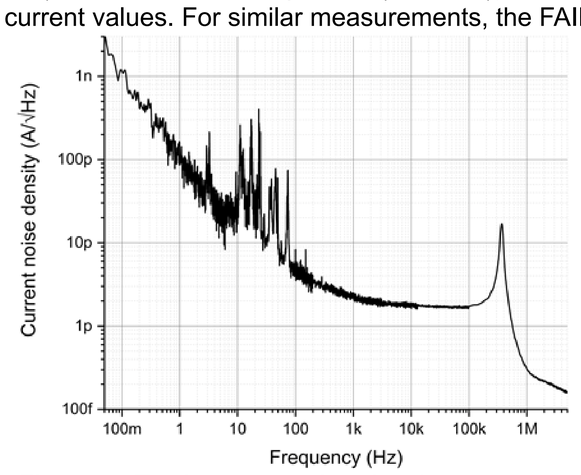

Figure 7: Total current noise density spectrum of the final DCCC-Sm-200, both pickup coils on one SQUID with input inductance of 1 µH.

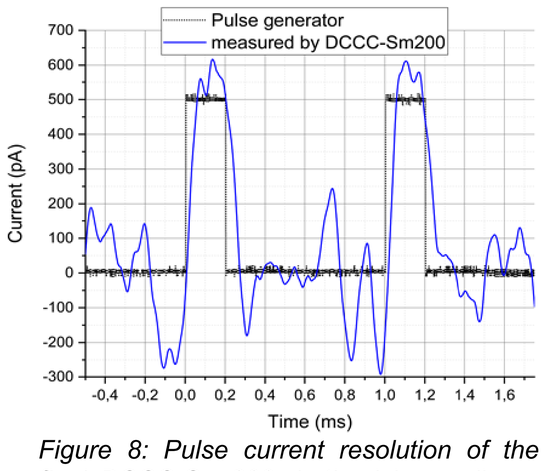

Figure 8: Pulse current resolution of the final DCCC-Sm-200, both pickup coils on one SQUID with input inductance of 1 µH.

Outlook

In the meantime, Magnetec has produced special cores that geometrically have the dimensions of M-616, but use the core material developed for the FAIR-Nb-CCC-XD with improved low-temperature properties. Thus, it is possible to achieve 13 % more inductance for the same geometry. With an additional core per pickup coil, the construction of the IFK-Pb-DCCC-Sm-300 could be started. It may have a total inductance 300 µH @ 4.2 K. The expected minimum white current noise density is accordingly 1.5 $pA_{rms}/\sqrt{Hz}$ – a similar R_s behavior assumed. Because of the expected better performance, the full final SQUID setup (two SQUIDs with L_i = 1 µH to reduce Barkhausen noise and increase system availability, one SQUID for dynamic expansion with L_i = 27 nH) and the installation into a new beam-line cryostat will probably no longer take place with Sm-200, but with the Sm-300.

References

[1] W. Vodel, R. Geithner and P. Seidel, “SQUID-Based Cryogenic Current Comparators”, in *Applied Superconductivity Handbook on Devices and Applications Volume 2*, P. Seidel, Ed. Weinheim, Germany: Wiley-VCH, 2015, pp. 1096-1110.

[2] M. Fernandes, “SQUID-Based Cryogenic Current Comparator for Measuring Low-Intensity Antiproton Beams”, Ph.D. thesis, University of Liverpool, UK, 2017.

[3] L. Crescimbeni *et al.*, “The Cryogenic Current Comparator at CRYRING@ESR”, presented at the 11th Int. Beam Instrumentation Conf. (IBIC’22), Krakow, Poland, Sept. 2022, paper TUP31, this conference.

[4] V. Tympel *et al.*, “First Measurements of a New Type of Coreless Cryogenic Current Comparators (4C) for Non-Destructive Intensity Diagnostics of Charged Particles” 8th Int. Beam Instrumentation Conf. (IBIC’19), Malmo, Sweden, Sept. 2019

[5] Magnetec, https://www.magnetec.de/wp-content/uploads/2018/11/m-616.pdf

[6] R. Geithner, “Optimierung eines kryogenen Stromkomparators für den Einsatz als Strahlmonitor”, Ph.D. thesis, Dept. Phys., F. Schiller University Jena, Jena, Germany, 2013.

Mail to volker.tympel@uni-jena.de

This project is supported by the BMBF, 05P15SJRBA & 05P18SJRB1, 05P18SJRB1.